Prell, W. L., Niitsuma, N., et al., 1991
Proceedings of the Ocean Drilling Program, Scientific Results, Vol. 117

25. LATE PLEISTOCENE SEA SURFACE WATER TEMPERATURE VARIATIONS OFF OMAN AS REVEALED BY THE DISTRIBUTION OF LONG-CHAIN ALKENONES[1]

H. L. ten Haven[2, 3] and D. Kroon[4, 5]

ABSTRACT

Late Pleistocene sea surface water temperatures (SST) offshore Oman were calculated from the $U^{k'}_{37}$ ratio measured in sediment extracts from ODP holes drilled on the Oman Margin (723B, 728B) and on the Owen Ridge (721B, 731A). The data revealed a complex history of SST variations with a temperature range of 18°/19°C–27°/28°C, which is in accord with the present-day SST range in the western Arabian Sea. We found that, notably, in the glacial periods of isotopic stages 3 and 8 the SST was lower than during the interglacials. The lowest SST values occurred during isotopic stage 3. A mechanism involving a strong influence of cold northeasterly winds during glacial periods, with the southwestern monsoon being less effective at the same time, explains cold SST during glacial periods. However, further research is necessary to approve or disapprove this mechanism, because in the present study not all glacial periods were clearly marked by low SST values.

INTRODUCTION

The major objective of Leg 117 was to study the environmental effects of the Indian Ocean monsoon as recorded in sediments deposited offshore Oman. At present, monsoonal winds seasonally change in direction; during the northern hemisphere winter near-surface winds blow from Asia over the Arabian Sea, whereas the wind direction is reversed during the summer. The driving force for this change in atmospheric circulation is cooling during the winter and heating during the summer of the Asian continent, resulting in a winter high-pressure cell and a summer low-pressure cell above the Tibetan Plateau. This changing wind pattern induces coastal upwelling along the coast of Oman and Somalia during a restricted period of the year. During the summer the southwesterly winds blow parallel to the coast, and Ekman transport causes offshore flow of surface waters, which are replaced by nutrient-rich, oxygen-poor cold water from several hundred meters depth. Changes in the intensity of these seasonal winds potentially have a large impact on the upwelling intensity, nutrient content, depth of the mixed-layer, sea surface water temperature (SST), and other oceanographic parameters (for a brief overview see Shipboard Scientific Party, 1989b, and references cited therein). Here, we want to focus on the changes in the SST during the late Pleistocene as determined by organic geochemical methods.

LONG-CHAIN ALKENONES AS POTENTIAL SST INDICATORS

Aquatic organisms are able to react to changes in water temperature to some extent by changing the molecular composition of the lipid bilayer of their membranes in order to maintain their fluidity. Indeed, Brassell et al. (1986a, b) noticed that the degree of unsaturation of long-chain alkenones in surface sediments varies with the SST and that the same parameter in more deeply buried sediments correlates well with variations in the $\delta^{18}O$ isotopic record of certain Pleistocene planktonic foraminifera, with a deterioration in sediments exceeding an age of 500 k.y.

The lipids in question, heptatriaconta-8E,15E,22E-trien-2-one ($C_{37:3}$) and heptatriaconta-15E,22E-dien-2-one ($C_{37:2}$), are major constituents of the coccolithophorid alga *Emiliania huxleyi* (Lohman) Hay and Mohler (Volkman et al., 1980; Prahl et al., 1988), but occur also in other species of the Class Prymnesiophyceae (Marlowe et al., 1984). However, the present-day scant knowledge of lipid distributions does not exclude the occurrence of alkenones in other marine organisms.

Brassell et al. (1986a) defined an alkenone unsaturation index, $U^{k}_{37} = (C_{37:2} - C_{37:4})/(C_{37:2} + C_{37:3} + C_{37:4})$, which can be simplified to $U^{k'}_{37} = C_{37:2}/(C_{37:2} + C_{37:3})$ for sediments where no $C_{37:4}$ occurs. High values (a low relative concentration of triunsaturated alkenones) correspond to warm surface waters, and low values to cold surface waters. Several studies have proven that this ratio correlates well with the SST (e.g., ten Haven et al., 1987; Prahl and Wakeham, 1987; Prahl et al., 1988; Poynter et al., 1989).

Laboratory culture experiments with *Emiliania huxleyi* have demonstrated an excellent relationship between the U^{k}_{37} ratio and the growth temperature, and a calibration curve to calculate SST was proposed (Prahl and Wakeham, 1987; Prahl et al., 1988). In the same studies, it was also shown that *Emiliania huxleyi* adjusts its lipid composition almost immediately in response to changing temperature. It is the widely accepted consensus that these lipids are transferred through the pelagic food chain and deposited in sediments without major alteration of their original composition (Corner et al., 1986; Prahl et al., 1988). Recently, Prahl et al. (1989) have shown that post-depositional oxidation of organic matter drastically reduces the absolute concentration of these alkenones, while the internal ratio (i.e. U^{k}_{37}) is hardly affected. This justifies their potential application as SST indicators, although perhaps not quantitatively accurate.

Previous studies of the U^{k}_{37} ratio as an indicator of SST variations, performed in upwelling areas offshore West Africa (Poynter et al., 1989) and offshore Peru (Farrington et al., 1988; Farrimond et al., 1990), gave results which could well be explained by variations of the SST. For instance, the high sedimentation rate offshore Peru and a close sampling density enabled Far-

---

[1] Prell, W. L., Niitsuma, N., et al., 1991. *Proc. ODP, Sci. Results*, 117: College Station, TX (Ocean Drilling Program).

[2] Institut für Erdöl and Organische Geochemie, KFA Jülich, Postfach 1913, D-5170 Jülich, Federal Republic of Germany.

[3] Present address: Institut Français du Pétrole, BP 311, F-92506 Rueil-Malmaison Cedex, France.

[4] Instituut voor Aardwetenschappen, Vrije Universiteit, Postbus 7161, NL-1007 MC Amsterdam, The Netherlands.

[5] Present address: Grant Institute of Geology, University of Edinburgh, West Mains Road, Edinburgh EH9 3JW, United Kingdom.

rington et al. (1988) to measure a U^k_{37} record which could be correlated to El Niño Southern Oscillation events, periods in which invasion of warm waters disturbs normal Peruvian upwelling conditions.

SAMPLES AND EXPERIMENTAL METHODS

Samples from late Pleistocene sections of four ODP sites were collected at 0.5 m intervals, because ODP policy did not allow a closer sampling density. Two sites (721, 731) are located on the Owen Ridge, and two sites (723, 728) on the Oman Margin underlying the area of present-day active upwelling during the northern hemisphere summer (Fig. 1). Sediments recovered from the Owen Ridge show a clear cyclicity as revealed by, inter alia, color and magnetic susceptibility. Light, medium, and dark-colored sediments were investigated.

Sediment samples from Holes 721B and 723B were extracted and analyzed on board the *JOIDES Resolution* (for analytical details see Shipboard Scientific Party, 1989a). Samples from Holes 728B and 731A were deep frozen until shore-based analysis. After thawing, an aliquot was taken for stable oxygen and carbon isotope analysis of the foraminifer *Neogloboquadrina dutertrei*. The methods of the stable oxygen and carbon isotope analysis are described by Steens et al. (this volume). The sample preparation techniques for organic geochemical studies, including carbon measurements, lipid extraction, derivatization, as well as instrumental conditions used for gas chromatography (GC) and gas chromatography-mass spectrometry (GC-MS) were identical to those described in the study of ODP Leg 112 samples (ten Haven et al., 1990). The U^k_{37} ratio was calculated from peak heights as measured with a VG Vax Multichrom GC data system. In order to eliminate erroneous results by coelution of other compounds, one sample was separated by high performance liquid chromatography in several fractions. The ketone plus ester fraction was saponified and further separated. The $U^{k'}_{37}$ ratio measured in the ketone fraction, thus obtained, showed a minimal difference (0.01) from the ratio measured on the total lipid fraction. The SST was calculated according to the equation $U^{k'}_{37} = 0.034T + 0.039$ (Prahl et al., 1988) with an estimated analytical accuracy of ± 0.5°C (Prahl and Wakeham, 1987). We noted a difference between shipboard and shore-based $U^{k'}_{37}$ measurements. The shipboard results are higher on average, but this difference is difficult to rationalize in terms of analytical artifacts. However, the widely-spaced sampling in combination with the high sedimentation rates offshore Oman hampers an accurate site to site correlation.

RESULTS AND DISCUSSION

In most samples the C_{37} alkenones are present as the most abundant free extractable lipids amenable to gas chromatography. Partial gas chromatograms of total lipid extracts of two samples from Hole 728B, showing the distribution of C_{37} and C_{38} alkenones, are given in Figure 2. The difference in U^k_{37} ratio (0.18) between these two samples corresponds to a SST difference of approximately 5°C.

Results of both shipboard and shore-based analyses are listed in Table 1, and several depth profiles are shown in Figures 3 to 6. The detailed oxygen stable isotope curve of Hole 728A (taken from Steens et al., this volume) was used as reference to date the SST variations, since the $\delta^{18}O$ values reflect both global ice volume and local SST changes. Steens et al. (this volume) recognized the isotopic stages and found that the isotope signal is predominantly determined by a global climatic signal. We used magnetic susceptibility data (Shipboard Scientific Party, 1989e) to correlate Hole 728A with Hole 728B (Fig. 4), because the SST variations were measured in sediment samples from the latter hole. The same procedure was applied to Site 723 (Fig. 5; magnetic susceptibility data from Shipboard Scientific Party, 1989d) except here the isotope stage boundaries were taken from

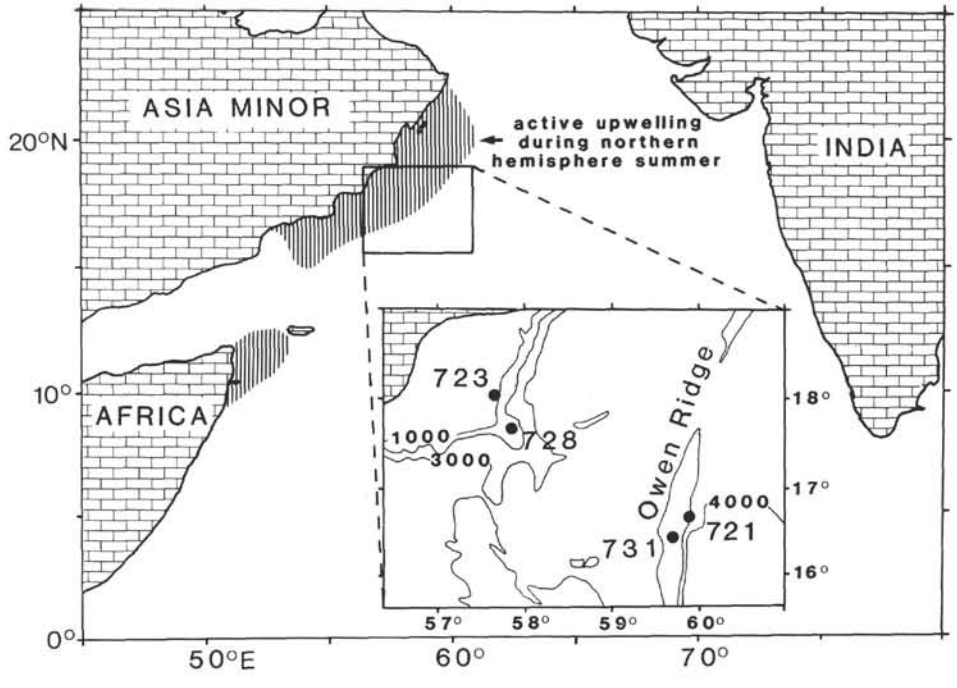

Figure 1. Location map of Sites 721, 723, 728, and 731 of ODP Leg 117 off the coast of Oman. Hole 721B: 16°40.636′N, 59°51.89′E (water depth 1944.8 m); Hole 723B: 18°03.079′N, 57°36.651′E (water depth 807.8 m); Hole 728B: 17°40.790′N, 57°49.553′E (water depth 1427.8 m; Hole 731A: 16°28.229′N, 59°42.149′E (water depth 2365.8 m).

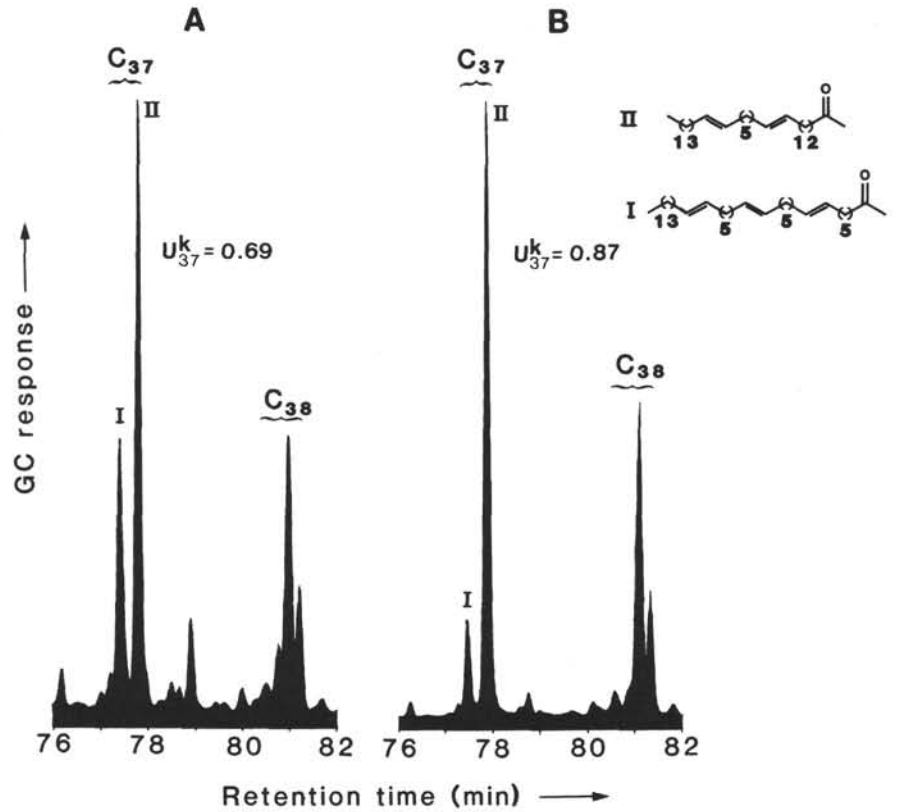

Figure 2. Partial gas chromatograms of the "total lipid" fractions of Sample 117-728B-2H-2, 79–82 cm (**A**), and Sample 728B-2H-6, 79–82 cm (**B**) showing the distribution of the C_{37} and C_{38} long-chain alkenones. The $U^{k'}_{37}$ ratios are 0.69 and 0.87, respectively. The structures of all-E $C_{37:3}$ (I) and $C_{37:2}$ (II) alkenones are shown with shorthand notation (cf. Rechka and Maxwell, 1988). The C_{38} cluster consists of di- and triunsaturated methyl and ethyl ketones.

the oxygen stable isotope curve measured by Niitsuma (this volume). An accurate stable isotope stratigraphy for Hole 731 was not available; therefore only rough estimates of the isotope stage boundaries could be made (Fig. 6).

Elevated C_{org} values measured in the Owen Ridge samples correspond to a dark coloration of the sediment, whereas low values (<0.5%) are found in light sections (Fig. 6). Generally, the C_{org} values of the Owen Ridge sediments are lower than those of the Oman Margin samples, as can be expected from the location of the Oman Margin drill sites in an area of present-day active upwelling and concomitant high primary bioproductivity.

The U^k_{37} record is thought to reflect the average local SST variations over at least a thousand years per sample (3 cm of sediment collected at intervals varying between 25 and 50 cm) taking an average sedimentation rate of 30 m/m.y. (see Prell, Niitsuma, et al., 1989 for reports on varying sedimentation rates). Thus, this ratio per sample includes the sedimentary expression of a thousand years of variations in monsoonal winds with periods of both warm and cold SST. Moreover, U^k_{37} is dependent on the relative productivity of Prymnesiophyceae during periods of upwelling (ca. 4 months/yr) and non-upwelling (ca. 8 months/yr), and the subsequent flux of alkenones to the sea bottom. Although quantitative alkenone measurements would indicate extended periods of intense upwelling, such data measured on samples of 3 cm would not discriminate the annual changes of upwelling and non-upwelling. Therefore, in this study no quantitative measurements were carried out.

The SST, as measured by the U^k_{37} ratio, varies between a lowest value of about 18°–19°C (measured at Sites 728 and 731) to a highest value of about 27°–28°C (Table 1). Presently, patches of SST values below 20°C occur over the shelf areas of Oman (Currie et al., 1973) and Somalia (Szekielda, 1987) during the southwest monsoon, whereas SST values of 26°–29°C are common for the central Arabian Sea (Prell and Streeter, 1982; Szekielda, 1987; Nair et al., 1989). Hence, the calculated sea surface temperatures are realistic in light of the present-day temperature range and are likely to indicate fluctuations in the past. Although the application of the U^k_{37} ratio as a quantitatively accurate SST indicator might be doubtful in "older" sediments due to the lack of a clear knowledge of the ecology of the organisms biosynthesizing these alkenones, we note that almost all samples investigated fall within the first occurrence zone of *Emiliania huxleyi,* presumably the major contributor of alkenones to sediments during the late Pleistocene. A study of Mediterranean sapropels (age range 8–225 k.y.) by ten Haven et al. (1987) indicated that the U^k_{37} ratio can indeed be used to unravel SST trends of late Pleistocene sediments.

Notably, low SST values were found for the glacial isotopic stages 3 and 8 in all holes (Figs. 3–6). The largest temperature drop (6°C) occurs between isotopic stages 5 to 3 in Hole 728B (Figs. 3, 4). A similarly low SST minimum as found in isotopic stage 3 of Hole 728B is observed at 0.79 mbsf in Hole 731A. This SST minimum probably also relates to the boundary between isotopic stages 3 and 4 (Fig. 6; there are no indications to attribute this isolated low SST value to an erroneous measure-

Table 1. Depth intervals and analytical results of sediment samples from Holes 721B, 723B, 728B, and 731A.

Core, section, interval (cm)	Depth (mbsf)	$CaCO_3$ (%)	C_{org} (%)	$U^{k'}_{37}$	SST (°C)	$\delta^{18}O$ (‰)	$\delta^{13}C$ (‰)
[a]117-721B-							
1H-2, 100–103	2.50	64.80	2.50	0.88	24.7	—	—
1H-4, 80–83	5.30	70.80	0.43	0.97	27.4	—	—
1H-5, 24–27	6.24	65.50	1.21	0.95	26.8	—	—
2H-1, 87–90	10.27	78.10	0.46	0.98	27.7	—	—
2H-2, 17–20	11.07	61.30	1.91	0.87	24.4	—	—
2H-3, 27–30	12.67	72.20	0.60	0.92	25.9	—	—
3H-3, 10–13	22.60	64.50	0.74	0.92	25.9	—	—
[b]117-723B-							
1H-1, 50–53	0.50	51.40	5.66	0.91	25.6	—	—
1H-2, 50–53	2.00	63.60	2.83	0.89	25.0	—	—
1H-3, 50–53	3.50	53.40	2.28	0.88	24.7	—	—
2H-1, 50–53	4.80	50.60	1.73	0.88	24.7	—	—
2H-1, 100–103	5.30	47.60	2.27	0.89	25.0	—	—
2H-2, 50–53	6.30	50.10	2.21	0.84	23.6	—	—
2H-2, 100–103	6.80	51.20	1.17	0.88	24.7	—	—
2H-3, 55–58	7.85	49.00	2.45	0.87	24.4	—	—
2H-3, 100–103	8.30	51.90	1.96	0.88	24.7	—	—
2H-4, 50–53	9.30	48.30	2.49	0.84	23.6	—	—
2H-4, 100–103	9.80	35.70	3.87	0.81	22.7	—	—
2H-5, 50–53	10.80	46.20	3.25	0.80	22.4	—	—
2H-5, 100–103	11.30	55.60	3.89	0.82	23.0	—	—
2H-6, 50–53	12.30	52.70	1.80	0.84	23.6	—	—
2H-6, 100–103	12.80	53.80	2.46	0.83	23.3	—	—
3H-1, 50–53	14.50	53.70	1.57	0.86	24.1	—	—
3H-1, 100–103	15.00	47.50	3.73	0.86	24.1	—	—
3H-2, 50–53	16.00	62.60	3.21	0.86	24.1	—	—
117-728B-							
1H-1, 14–17	0.14	68.89	1.80	0.90	25.3	−0.71	1.16
1H-1, 53–56	0.53	76.64	0.84	0.87	24.3	0.16	0.93
1H-1, 83–86	0.83	55.48	0.47	0.82	23.0	1.32	1.05
2H-1, 35–38	1.55	60.06	1.18	0.83	23.2	0.74	0.81
2H-1, 79–82	1.99	60.31	1.08	0.85	23.8	0.64	1.10
2H-1, 119–122	2.39	60.89	1.36	0.80	22.5	0.66	1.04
2H-2, 35–38	3.05	64.81	1.35	0.72	20.0	0.29	0.85
2H-2, 79–82	3.49	61.06	1.14	0.69	19.2	0.26	0.61
2H-2, 119–122	3.89	59.81	0.87	0.72	19.9	0.52	1.08
2H-3, 35–38	4.55	65.22	0.88	0.78	21.8	—	—
2H-3, 79–82	4.99	64.31	1.21	0.82	22.9	−0.15	1.09
2H-3, 119–122	5.39	64.47	1.49	0.84	23.6	—	—
2H-4, 35–38	6.05	64.56	1.03	0.80	22.4	0.93	0.39
2H-4, 79–82	6.49	57.14	0.99	0.83	23.2	0.32	1.17
2H-4, 119–122	6.89	54.89	0.99	0.83	23.2	0.41	0.76
2H-5, 35–38	7.55	59.31	0.71	0.84	23.5	0.42	0.71
2H-5, 82–85	8.02	54.98	0.47	0.82	23.0	0.73	0.64
2H-5, 122–125	8.42	51.98	0.87	0.86	24.2	—	—
2H-6, 35–38	9.05	51.98	0.85	0.85	23.7	1.00	0.55
2H-6, 79–82	9.49	58.98	1.08	0.87	24.3	0.18	0.62
2H-6, 119–122	9.89	56.39	0.83	0.87	24.5	0.20	0.44
2H-7, 18–21	10.38	59.39	1.39	0.92	25.9	0.30	0.90
2H-7, 69–72	10.89	66.31	1.34	0.89	24.9	−0.28	0.94
3H-1, 29–32	10.99	71.05	1.27	0.86	24.2	−0.52	0.25
3H-1, 71–74	11.41	59.39	0.50	0.82	22.9	0.82	0.25
3H-1, 109–122	11.79	60.89	1.03	0.90	25.3	−0.02	0.78
3H-2, 29–32	12.49	58.81	1.10	0.82	22.9	0.15	0.50
3H-2, 71–74	12.91	58.23	1.39	0.79	21.9	0.38	0.37
3H-2, 109–112	13.19	59.23	1.26	0.80	22.2	0.35	0.62
3H-3, 29–32	13.99	58.81	0.42	0.80	22.2	1.14	0.76
117-731A-							
1H-1, 35–38	0.35	58.64	0.47	0.84	23.7	—	—
1H-1, 56–59	0.56	66.22	1.26	0.85	23.7	0.53	0.82
1H-1, 79–82	0.79	59.23	0.68	0.65	18.0	0.60	0.82
1H-1, 102–105	1.02	67.97	1.30	0.81	22.6	0.27	0.96
1H-1, 122–125	1.22	66.81	0.48	0.79	22.2	0.50	0.97
1H-2, 32–35	1.82	59.31	0.38	0.83	23.2	0.76	1.09
1H-2, 71–74	2.23	64.72	0.84	0.82	23.0	0.00	1.19
1H-2, 102–105	2.52	59.48	0.33	0.85	23.7	—	—
1H-2, 119–122	2.69	70.64	1.01	0.87	24.5	0.03	1.36
1H-3, 113–116	4.13	64.14	0.47	0.87	24.5	0.70	0.57
1H-3, 132–135	4.32	61.64	0.71	0.84	23.5	0.75	0.56
1H-4, 11–14	4.61	64.64	0.91	0.86	24.2	0.80	0.87

Table 1 (continued).

Core, section, interval (cm)	Depth (mbsf)	$CaCO_3$ (%)	C_{org} (%)	$U^{k'}_{37}$	SST (°C)	$\delta^{18}O$ (‰)	$\delta^{13}C$ (‰)
117-731A- (Cont.)							
1H-4, 56–59	5.05	64.06	0.46	0.85	23.8	0.73	0.87
1H-4, 124–127	5.75	53.31	0.59	0.82	23.1	0.71	0.61
1H-5, 26–29	6.26	57.23	0.82	0.83	23.2	0.40	0.99
1H-5, 69–72	6.69	55.39	0.38	0.83	23.2	—	—
1H-5, 128–131	7.28	56.73	0.75	0.83	23.4	0.39	0.87
1H-6, 12–15	7.62	72.89	0.36	0.87	24.4	−0.29	1.05
1H-6, 55–58	8.05	71.80	0.57	0.82	22.9	−0.35	1.01
1H-6, 103–106	8.57	58.14	0.23	0.81	22.7	—	—
1H-7, 7–10	9.07	75.05	0.59	0.89	24.9	−0.31	1.00
1H-7, 28–30	9.28	65.14	0.29	0.84	23.7	0.19	0.38
1H-7, 50–53	9.50	66.06	0.58	0.87	24.5	0.32	0.44
2H-1, 27–30	10.07	67.14	0.58	0.78	21.8	0.36	0.55
2H-1, 52–55	10.32	63.72	0.84	0.82	22.8	0.28	0.68
2H-1, 71–74	10.51	65.72	0.56	0.79	22.2	0.78	0.76

[a] Data from Shipboard Scientific Party (1989c).
[b] Data from Shipboard Scientific Party (1989d).

ment). SST variations in Hole 723B show the same trends as observed in Hole 728B, although the SST minimum in early isotopic stage 3 is less pronounced than in Hole 728B (Fig. 6). A follow-up research with more closely spaced samples may show a larger temperature drop, however.

No straightforward correlation was observed between the parameters measured ($\delta^{18}O$, $\delta^{13}C$, $U^{k'}_{37}$, C_{org}, $CaCO_3$). The lack of correlation between SST and the $CaCO_3$ or C_{org} content is understandable considering that relative carbon percentages depend on sedimentation rates and low values merely may indicate dilution effects by windblown and other transported material. The lack of correlation between SST and $\delta^{18}O$ values is not surprising either, because the latter values are a reflection of both local SST variations and global ice-volumes. These local SST variations do not necessarily correlate with global climate variations expressed as variation of stable oxygen isotopes linked with ice volume changes.

In contrast to the present-day offshore gradient in SST, no significant difference exists between the Oman Margin and the Owen Ridge sites, although the margin holes are closer to the upwelling centers where deep cold waters are driven to the surface. Although the highest SST values were measured at Site 721 on the Owen Ridge, we do not consider these results significant at this stage of research because of the lower SST values at Site 731 (also Owen Ridge) and the lack of layer-to-layer correlation between sediments deposited on the Oman Margin and on the Owen Ridge.

Also, the fact that the $U^{k'}_{37}$ ratios in samples from some glacial periods point to lower temperatures is surprising at first, because diagnostic upwelling biota assemblages suggest that upwelling intensity was stronger during the interglacials. These latter parameters thus respond to time spans with increased northern hemisphere solar radiation during which a larger land-ocean pressure gradient induced stronger upwelling (Prell et al., 1980; Shimmield, this volume; Steens et al., this volume). Prell and Kutzbach (1987) estimated the strongest monsoonal winds to occur during isotopic stage 5 applying model calculations to simulate one season over an extended period of time. Hence, a mechanism other than monsoonal upwelling variations may be needed to explain the lower SST values during the glacial periods (notably during isotopic stages 3 and 8) in the western Arabian Sea. The effect of this mechanism must have been even greater than the upwelling-induced temperature variations, because upwelling was stronger during the interglacials with lower SST values during the summer. We note that Zahn and Pedersen (this vol-

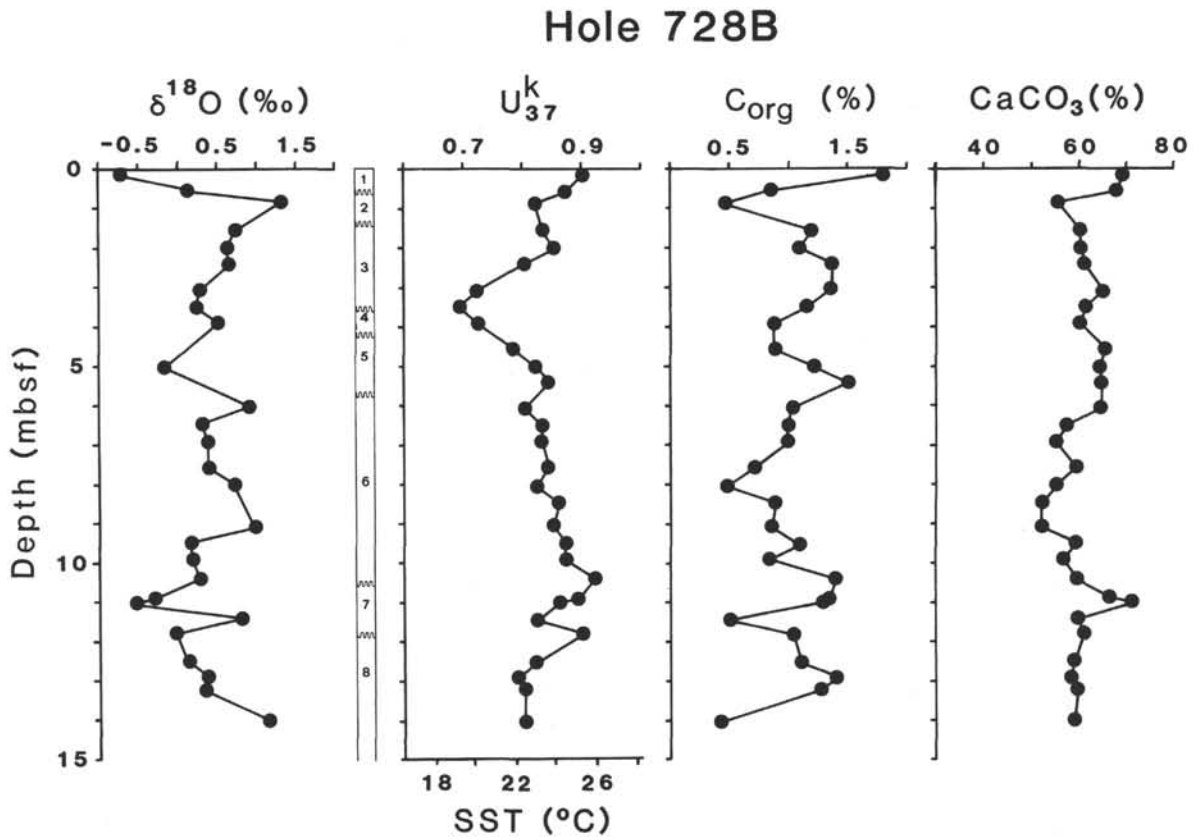

Figure 3. Depth profiles in Hole 728B of $\delta^{18}O$ values measured in *Neogloboquadrina dutertrei* and the inferred isotope stratigraphy (see also Fig. 4), the U^{k}_{37} ratio of sediment extracts, and the C_{org} and $CaCO_3$ content of sediments. The sea surface water temperature (SST) is calculated according to Prahl et al. (1988).

ume), applying different techniques, also came to the conclusion that SST values were lower during glacial periods.

A plausible mechanism may be that the winter sea surface water temperatures were lower during the glacial periods than at present because of strengthened northeasterly winds. These winds were indeed stronger as evidenced by a pollen record from the western Arabian Sea (van Campo et al., 1982) and by desert dunes formed during the last glacial maximum (Goudie et al., 1973; Verstappen, 1970; Singh et al., 1972). An expanded ice sheet on the Tibetan Plateau cooled off the region and the northeasterly winds subsequently cooled the Arabian Sea. In addition, stronger winds deepened the mixed-layer during the glacial winter seasons (cf. Nair et al., 1989). In this mechanism the southwestern monsoon was weakened during the glacial periods, and colder SST values occurred in the western Arabian Sea due to strengthened northeasterly winds. However, this mechanism fails to explain why "extremely" low SST values were recorded in glacial isotopic stage 3, which are not found to a similar extent in other glacial periods. It is evident that a more detailed follow-up study (applying a much closer sampling density) is needed in order to find out whether the proposed mechanism above is realistic or if we are dealing with a curious anomaly during isotopic stage 3.

ACKNOWLEDGMENTS

Samples were obtained through the assistance of the international Ocean Drilling Program. We thank M. Radke for providing laboratory facilities, G. Beltz for analytical support, and B. Boekschoten and J. Rullkötter for reading a first version of the manuscript. We gratefully acknowledge the critical reviews of L. Sykes, W. L. Prell, and a "known" anonymous referee. The research was supported by the Deutsche Forschungsgemeinschaft (DFG; grant We 346/27) and the Nederlandse Organisatie voor Wetenschappelijk Onderzoek (NWO; grant 751-356-018) and the Stichting Onderzoek der Zee (SOZ).

REFERENCES

Brassell, S. C., Brereton, R. G., Eglinton, G., Grimalt, J., Liebezeit, G., Marlowe, I. T., Pfaumann, U., and Sarnthein, M., 1986. Palaeoclimatic signals recognised by chemometric treatment of molecular stratigraphic data. *In* Leythaeuser, D., and Rullkötter, J. (Eds.), *Advances in Organic Geochemistry 1985.* Org. Geochem., 10:649–660.

Brassell, S. C., Eglinton, G., Marlowe, I. T., Pflaumann, U., and Sarnthein, M., 1986b. Molecular stratigraphy: a new tool for climatic assessment. *Nature,* 320:129–133.

Corner, E.D.S., O'Hara, S.C.M., Neal, A. C., and Eglinton, G., 1986. Copepod faecal pellets and the vertical flux of biolipids. *In* Corner, E.D.S., and O'Hara, S.C.M. (Eds.), *The Biological Chemistry of Marine Copepods:* Oxford (Science Publications), 260–321.

Currie, R. I., Fisher, A. E., and Hargraves, P. M., 1973. Arabian Sea upwelling. *In* Zeitzschel, B., and Gerlach, S. A. (Eds.), *The Biology of the Indian Ocean* (Vol. 3): New York (Springer-Verlag), 37–52.

Farrimond, P., Poynter, J. G., and Eglinton, G., 1990. A molecular stratigraphic study of Peru margin sediments, Hole 686B, Leg 112. *In* Suess, E., von Huene, R., et al., *Proc. ODP, Sci. Results,* 112: College Station, TX (Ocean Drilling Program), 547–553.

Farrington, J. W., Davis, A. C., Sulanowski, J., McCaffrey, M. A., McCarthy, M., Clifford, C. H., Dickinson, P., and Volkman, J. K., 1988. Biochemistry of lipids in surface sediments of the Peru upwelling area at 15°S. *In* Mattavelli, L., and Novelli, L. (Eds.), *Advances in Organic Geochemistry 1987.* Org. Geochem., 13:607–617.

Goudie, A. S., Allchin, B., and Hedge, K.T.M., 1973. The former extensions of the Great Indian desert. *Geogr. J.,* 139:243–257.

Marlowe, I. T., Brassell, S. C., Eglinton, G., and Green, J. C., 1984. Long-chain unsaturated ketones and esters in living algae and marine sediments. *In* Schenck, P. A., de Leeuw, J. W., and Lijmbach, G.W.M. (Eds.), *Advances in Organic Geochemistry 1983*. Org. Geochem., 6:135–141.

Nair, R. R., Ittekkot, V., Manganini, S. J., Ramaswamy, V., Haake, B., Degens, E. T., Desai, B. N., and Honjo, S., 1989. Increased particle flux to the deep ocean related to monsoons. *Nature,* 338:749–751.

Poynter, J. G., Farrimond, P., Brassell, S. C., and Eglinton, G., 1989. A molecular stratigraphic study of sediments from Holes 658A and 660A, ODP Leg 108. *In* Ruddiman, W., Sarnthein, M., et al., *Proc. ODP, Sci. Results,* 108: College Station, TX (Ocean Drilling Program), 387–394.

Prahl, F. G., de Lange, G. J., Lyle, M., and Sparrow, M. A., 1989. Post-depositional stability of long-chain alkenones under contrasting redox conditions. *Nature,* 341:434–437.

Prahl, F. G., Muehlhausen, A., and Zahnle, D., 1988. Further evaluation of long-chain alkenones as indicators of paleoceanographic conditions. *Geochim. Cosmochim. Acta,* 52:2303–2310.

Prahl, F. G., and Wakeham, S. G., 1987. Calibration of unsaturation patterns in long-chain ketone compositions for palaeotemperature assessment. *Nature,* 330:367–369.

Prell, W. L., Hutson, W. H., William, D. F., Be, A.W.H., Geitzenauer, R., and Molfino, B., 1980. Surface circulation of the Indian Ocean during the last interglacial maximum, approximately 18,000 yr. B.P. *Quat. Res.,* 14:309–336.

Prell, W. L., and Kutzbach, J. E., 1987. Monsoon variability over the past 150,000 years. *J. Geophys. Res.,* 92:8411–8425.

Prell, W. L., Niitsuma, N., et al., 1989. *Proc. ODP, Init. Repts,* 117: College Station, TX (Ocean Drilling Program).

Prell, W. L., and Streeter, H. F., 1982. Temporal and spatial patterns of monsoonal upwelling along Arabia: a modern analogue for the interpretation of Quaternary SST anomalies. *J. Mar. Res.,* 40:143–155.

Rechka, J. A., and Maxwell, J. R., 1988. Characterisation of alkenone temperature indicators in sediments and organisms. *In* Mattavelli, L., and Novelli, L. (Eds.), *Advances in Organic Geochemistry 1987.* Org. Geochem., 13:727–734.

Shipboard Scientific Party, 1989a. Explanatory Notes. *In* Prell, W. L., Niitsuma, N., et al., *Proc. ODP, Init. Repts.,* 117: College Station, TX (Ocean Drilling Program), 11–34.

_____, 1989b. Introduction, background, and major objectives for ODP Leg 117 (western Arabian Sea) in search of ancient monsoons. *In* Prell, W. L., Niitsuma, N., et al., *Proc. ODP, Init. Repts.,* 117: College Station, TX (Ocean Drilling Program), 5–10.

_____, 1989c. Site 721. *In* Prell, W. L., Niitsuma, N., et al., *Proc. ODP, Init. Repts.,* 117: College Station, TX (Ocean Drilling Program), 197–254.

_____, 1989d. Site 723. *In* Prell, W. L., Niitsuma, N., et al., *Proc. ODP, Init. Repts.,* 117: College Station, TX (Ocean Drilling Program), 319–384.

_____, 1989e. Site 728. *In* Prell, W. L., Niitsuma, N., et al., *Proc. ODP, Init. Repts.,* 117: College Station, TX (Ocean Drilling Program), 495–546.

Singh, G., Joshi, R. D., and Singh, A. B., 1972. Stratigraphic and radiocarbon evidence for the age and development of three salt lake deposits in Rajasthan, India. *Quat. Res.,* 2:496–505.

Szekielda, K. H., 1987. Investigations with satellites on eothrophication of coastal regions. Part VII: response of the Somali upwelling onto monsoonal changes. *In* Degens, E. T., Kempe, S., and Naidu, S. A. (Eds.), *Transport of Carbon and Minerals in Major World Rivers.* SCOPE/UNEP Sonderband, Mitt. Geol. Paläont. Inst. Univ. Hamburg, 66:1–30.

ten Haven, H. L., Baas, M., Kroot, M., de Leeuw, J. W., Schenck, P. A., and Ebbing, J., 1987. Late Quaternary Mediterranean sapropels: III. Assessment of source of input and palaeotemperature as derived from biological markers. *Geochim. Cosmochim. Acta,* 51: 803–810.

ten Haven, H. L., Littke, R., Rullkötter, J., Stein, R., and Welte, D. H., 1990. Accumulation rates and composition of organic matter in late Cenozoic sediments underlying the active upwelling area off Peru. *In* Suess, E., von Huene, R., et al., *Proc. ODP, Sci. Results,* 112: College Station, TX (Ocean Drilling Program), 591–606.

Van Campo, E., Duplessy, J. C., and Rossignol-Strick, M., 1982. Climatic conditions deduced from a 150-kyr oxygen isotope-pollen record from the Arabian Sea. *Nature,* 296:56–59.

Verstappen, H. T., 1970. Aeolian geomorphology of the Thar Desert and palaeoclimates. *Z. Geomorphol. Suppl.,* 10:104–120.

Volkman, J. K., Eglinton, G., Corner, E.D.S., and Sargent, J. R., 1980. Novel unsaturated straight-chain C_{37}–C_{39} methyl and ethyl ketones in marine sediments and a coccolithophore *Emiliania huxleyi. In* Douglas, A. G., and Maxwell, J. R. (Eds.), *Advances in Organic Geochemistry 1979:* Oxford (Pergamon Press), 219–228.

Date of initial receipt: 1 September 1989
Date of acceptance: 8 May 1990
Ms 117B-159

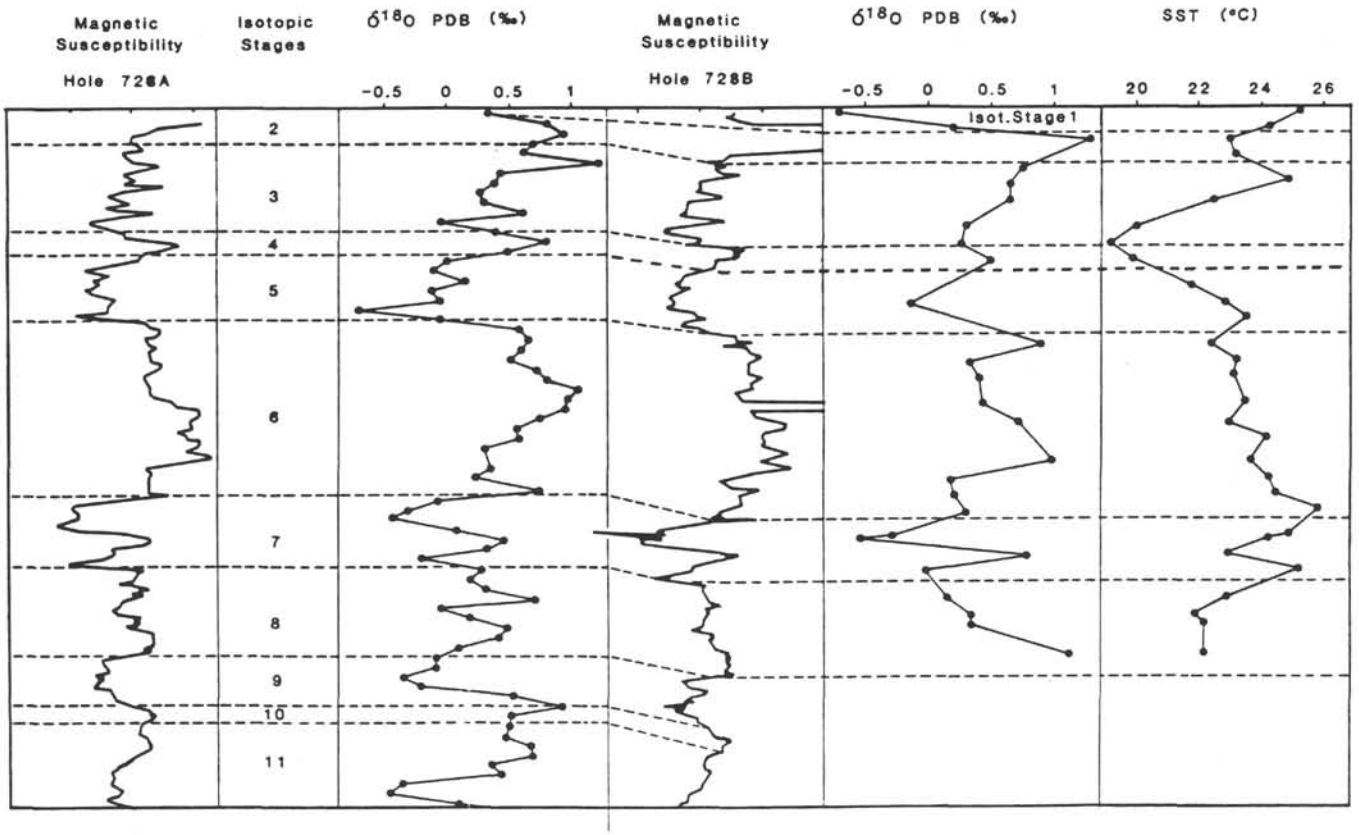

Figure 4. Correlation of Hole 728A with Hole 728B using magnetic susceptibility and calculated SST (see also Fig. 3).

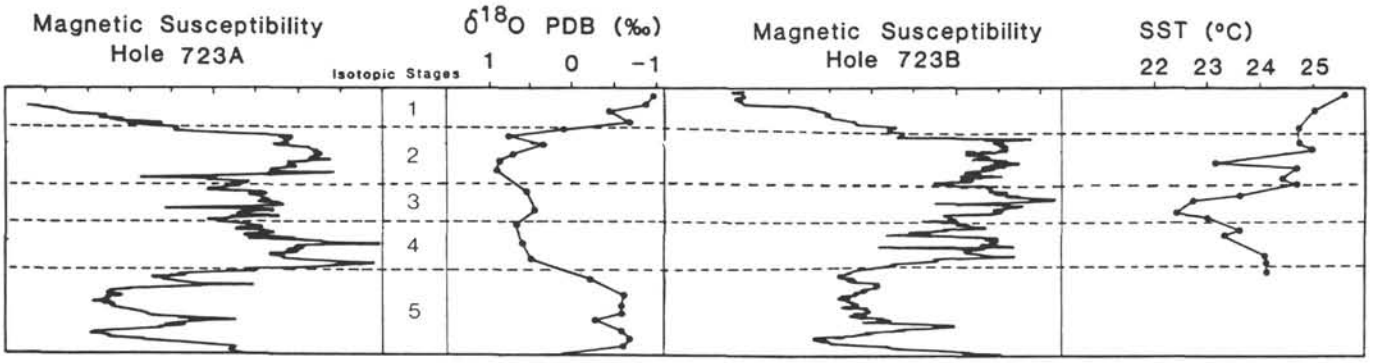

Figure 5. Correlation of Hole 723A with Hole 723B using magnetic susceptibility and calculated SST. Isotope stratigraphy is taken from Niitsuma (this volume).

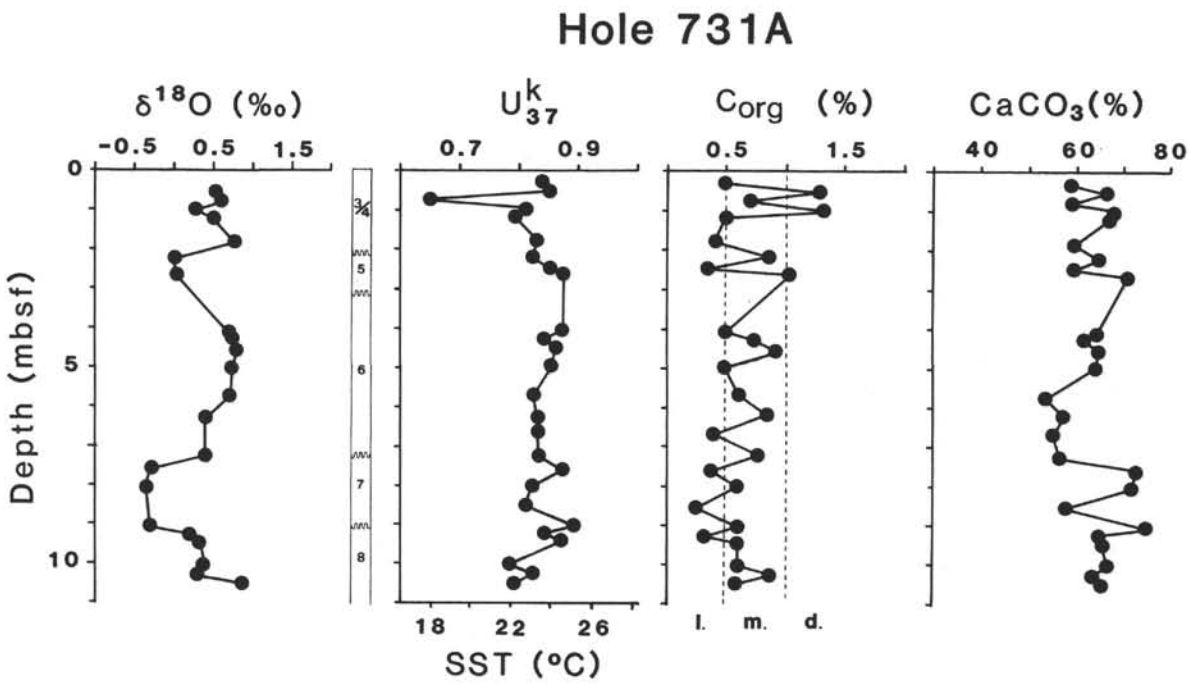

Figure 6. Depth profiles in Hole 731A of $\delta^{18}O$ values measured in *Neogloboquadrina dutertrei* and the inferred isotope stratigraphy, the $U^{k'}_{37}$ ratio of sediment extracts, and the C_{org} and $CaCO_3$ content of sediments. The color gradation (light, medium, dark) of the sediments is indicated in the C_{org} profile.